Available online at www.sciencedirect.com
ScienceDirect
Trans. Nonferrous Met. Soc. China 25(2015) 1122−1127
Transactions of Nonferrous Metals Society of China
www.tnmsc.cn

Facile hydrothermal synthesis of TiO_2−CaP nano-films on Ti6Al4V alloy

Tao FU[1], Hong-wei LI[2], Jian-min SUN[1], Gang LI[3], Wen LI[2], Hong-mei ZHANG[1]

1. Key Laboratory of Biomedical Information Engineering of Ministry of Education, School of Life Science and Technology, Xi'an Jiaotong University, Xi'an 710049, China;
2. School of Materials Science and Engineering, Chang'an University, Xi'an 710064, China;
3. State Key Laboratory of Porous Metal Materials, Northwest Institute for Nonferrous Metal Research, Xi'an 710016, China

Received 12 May 2014; accepted 31 July 2014

Abstract: Ti6Al4V alloy was subjected to hydrothermal treatment in the concentrated $Ca_3(PO_4)_2$, $CaHPO_4$ and $Ca(H_2PO_4)_2$ solutions for bioactive surface modification. The treated samples are covered by films composed of nano-particles with the size of 60−240 nm. Such film can also be grown on the strut surface of a Ti6Al4V scaffold prepared by electron beam melting (EBM) technology. XPS analysis indicates that Ti element on the surface presents as TiO_2, and Ca and P elements are in the form of calcium phosphate. XRD and Raman analyses show that the surface layer is composed of anatase TiO_2 and hydroxyapatite. Potentiodynamic polarization test in a Ca-free Hank's balanced solution demonstrates that the treated sample has markedly improved corrosion resistance compared with the polished sample. The present work provides a bioactive surface modification method that is easily-operated, low-temperature, less corrosion, and applicable to porous Ti6Al4V alloy for biomedical applications.
Key words: titanium; TiO_2; calcium phosphate; hydrothermal treatment; corrosion

1 Introduction

Due to its low density and excellent mechanical properties, Ti6Al4V alloy has been utilized to manufacture various implants especially in orthopedic fields. In order to avoid "stress shielding" of metallic implants, porous titanium and low modulus titanium alloys are being developed. The methods for preparing porous titanium and other metallic scaffolds include space-holder sintering, replication dip coating, combustion synthesis, laser engineering net shaping (LENS), electron beam melting (EBM), etc [1−5]. In EBM processing, physical parts are fabricated by melting metal powder layer by layer with an electron beam according to the CAD data [6,7]. Compared with the laser-based additive manufacturing techniques [5], EBM has the advantage of producing small parts with complicated shapes.

The bioactive surface modification of porous titanium (with pore size of tens or hundreds of micrometers) becomes an interesting topic in recent years [8−11]. The modification layer on the open pore walls should be even in thickness. The surface modification methods are also required not to seriously influence intrinsic properties of the porous metals. For example, the well-known alkali-heat treatment can induce bioactivity for titanium and Ti alloys [10,11], but it has drawbacks in surface modification of porous titanium metals. The corrosion of alkali solution was reported to have an adverse effect on porous titanium, with the mechanical properties deteriorated [10]. Heat treatment alters microstructure and may vary mechanical properties of special alloys [11−13]. Therefore, new methods have to be developed for bioactive surface modification of porous titanium and its alloys.

Hydrothermal treatment is an easily-operated and low-temperature method for surface modification of titanium metals. Since the modification layer is in nanometer thickness, only small quantities of solute and solvent are consumed. The high pressure environment can greatly accelerate diffusion of the reactants.

Foundation item: Projects (xjj2011096, CHD2011JC001) supported by the Fundamental Research Fund for the Central Universities, China; Projects (50901058, 51374174) supported by the National Natural Science Foundation of China; Project (2013JZ015) supported by the Science and Technology Program of Shaanxi Province, China
Corresponding author: Tao FU; Tel: +86-29-82669021; E-mail: taofu@mail.xjtu.edu.cn
DOI: 10.1016/S1003-6326(15)63706-2

$Ca(OH)_2$, $CaCl_2$ and $MgCl_2$ solutions were used to surface-modify Ti and TiNb alloy, with better bioactivity and osteoblast cell growth obtained [13−16]. The shortcomings of these methods are that the solutions have corrosive effect on titanium during the hydrothermal treatment, and the formed films only contain Ca or Mg, without phosphate. In this work, a facile hydrothermal method was presented to grow TiO_2−calcium phosphate (CaP) nano-films on Ti6Al4V alloy and its scaffold. Surface structure, chemical composition and corrosion resistance of the treated alloy samples were investigated.

2 Experimental

Ti6Al4V alloy plates (9 mm × 12 mm × 2 mm) were polished with SiC paper down to grits 1200, ultrasonically cleaned in acetone, ethanol, deionized (DI) water in sequence, and dried in air. The polished samples were hydrothermally treated in the solutions of $Ca_3(PO_4)_2$, $CaHPO_4$ and $Ca(H_2PO_4)_2$ with concentrations of 3.3, 10 and 10 mmol/L, respectively. The filling ratio of solution in the Teflon-lined autoclave was about 4:5. The sample stood vertically in the autoclave with the help of a titanium clamp. The autoclave was sealed and heated at 200 °C for different time (Table 1). After the treatment, the samples were evacuated and rinsed with deionized water several times and dried for analyses.

Table 1 Solute and hydrothermal parameters for Ti6Al4V samples

Sample	Solute	Parameter
SA-16h	$Ca_3(PO_4)_2$, 3.3 mmol/L	200 °C, 16 h
SB-16h	$CaHPO_4{\cdot}2H_2O$, 10 mmol/L	200 °C, 16 h
SB-24h	$CaHPO_4{\cdot}2H_2O$, 10 mmol/L	200 °C, 24 h
SB-72h	$CaHPO_4{\cdot}2H_2O$, 10 mmol/L	200 °C, 72 h
SC-16h	$Ca(H_2PO_4)_2$, 10 mmol/L	200 °C, 16 h

Surface morphology of the samples was analyzed with a scanning electron microscope (SEM, FEI Quanta 600F) equipped with the energy dispersive analysis of X-ray (EDX), and microstructure was examined by X-ray diffraction (XRD, Cu K_α, X'Pert PRO) and Raman scattering (Horiba HR 800, 633 nm). Elemental composition and chemical bonding state of the samples were examined by X-ray photoelectron spectroscopy (XPS, Al K_α, VG). Corrosion resistance of the samples was evaluated by potentiodynamic polarization tests in a Ca-free Hank's balanced salt solution (HBSS, 8.00 g/L NaCl, 0.40 g/L KCl, 0.34 g/L $NaHCO_3$, 0.06 g/L KH_2PO_4, 0.12 g/L $Na_2HPO_4{\cdot}12H_2O$) by using an electrochemical workstation (Model CS150, Corrtest®) under ambient conditions. A platinum electrode was used as counter electrode, and the saturated calomel electrode (SCE) was reference electrode.

3 Results and discussion

3.1 Surface morphology and elemental analysis

Surface micrographs of the hydrothermally-treated Ti6Al4V alloy samples are shown in Fig. 1. The surface of the sample treated in $Ca_3(PO_4)_2$ solution is rough at nano-scale, and the sample treated in $CaHPO_4$ solution is covered by a dense nano-particle film (size ~60 nm). For the sample treated in $Ca(H_2PO_4)_2$ solution, there are small particles (50−100 nm) and large particles (~240 nm) on the surface. TiO_2 nano-grains can be hydrothermally prepared on Ti substrate through a dissolution−precipitation mechanism [15]. For the third sample, Ca and P elements were detected by EDX analysis, with mole fraction of Ca of 0.16% and mole fraction of P of 0.61%. The particles on the sample surface are presumed to be TiO_2 and calcium phosphate. Water contact angles of the three samples are 101°, 69° and 51°, respectively. The smallest contact angle of sample SC-16h is possibly related to its high content of hydrophilic calcium phosphate deposited on the surface as a result of the highest solubility of $Ca(H_2PO_4)_2$ among the three calcium phosphates (Table 2).

Sample SB-24h was treated at a longer duration (24 h), and the particles grew larger than those of sample SB-16h (Figs. 1(b) and (d)). Since sample SB-24h has large and even grain size due to the enough treatment duration and appropriate solubility of $CaHPO_4$, its hydrothermal parameters were used to treat a Ti6Al4V scaffold produced by EBM technology [7]. It can be seen from Fig. 2 that the same nano-films are formed on the strut surface after the hydrothermal treatment.

Surface chemical composition of sample SB-24h was examined by XPS, with the Ti 2p, Ca 2p, P 2p, Al 2p, V 2p and O 1s spectra shown in Fig. 3. Titanium on the sample surface presents mainly in the form of TiO_2, having the binding energies of 464.1 eV (Ti $2p_{1/2}$) and 458.5 eV (Ti $2p_{3/2}$). The Ca 2p peaks (350.9 and 347.3 eV) and P 2p peak (133.3 eV) confirm that calcium phosphate is formed on the sample surface [17]. According to the studies on hydrothermally-treated Ti [14,16], calcium compounds (titanate, carbonate or hydroxide) can also be formed in Ca^{2+}-containing solutions. The alloy elements of Al and V are still detectable, but their signals are fairly weak. The Al 2p and V 2p peaks indicate that they exist as oxides (Al_2O_3 and VO_2 [18]) on the sample surface. In the O 1s spectra, the main peak at 529.8−530.0 eV is attributed to TiO_2. The peak related to calcium phosphate (531.2 eV [17]) lies in the left shoulder area. This peak is more apparent for the spectrum before sputtering. The small peak of hydroxyl groups is positioned at even higher binding energy (532.0 eV).

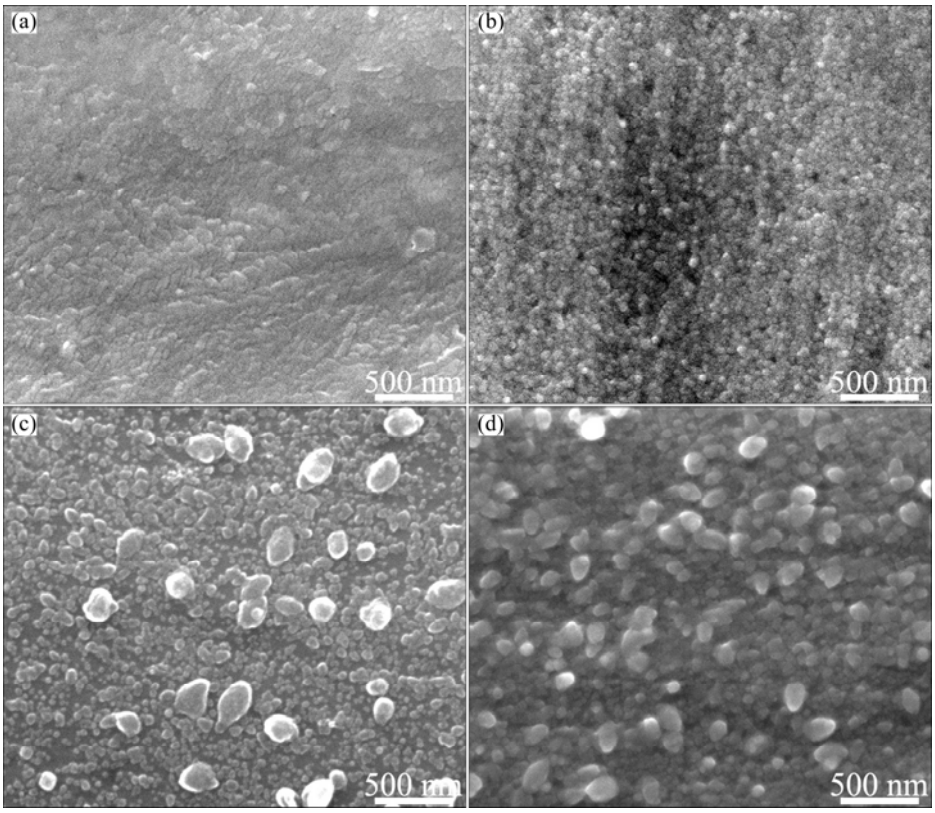

Fig. 1 SEM micrographs of hydrothermally-treated Ti6Al4V samples: (a) SA-16h; (b) SB-16h; (c) SC-16h; (d) SB-24h

Table 2 Solubility values of calcium phosphates at 20 °C

Calcium phosphate	Solubility/(g·mL^{-1})
$Ca_3(PO_4)_2$	2.0×10^{-5}
$CaHPO_4$	4.3×10^{-5}
$Ca(H_2PO_4)_2$	1.8×10^{-2}

3.2 Crystallography analysis

Grazing-angle XRD patterns of the samples SB-16h and SB-24h are shown in Fig. 4. The diffraction peaks of the alloy substrate and the weak anatase peak at 2θ=25.2° are present for sample SB-24h, although calcium phosphate is detected by XPS.

Microstructure of the surface layer of the hydrothermally-treated sample was further studied by Raman analysis (Fig. 5). The peaks at 147, 198, 394, 515 and 636 cm^{-1} are indicative of anatase TiO_2 layer formed on the sample surface [19]. The weak peak located at 965 cm^{-1} is due to the ν_1 symmetric stretching of the P—O mode, which is the characteristic peak from hydroxyapatite [20,21]. There are other three vibration modes for phosphate apatite [20]: the symmetric O—P—O bending mode (ν_2) at around 430−450 cm^{-1}; the asymmetric O—P—O bending mode (ν_4) at 580−630 cm^{-1}; and ν_3 mode at around 1050 cm^{-1}. The frequency ascribed to the first mode is observable as the small peak is located at 451 cm^{-1}.

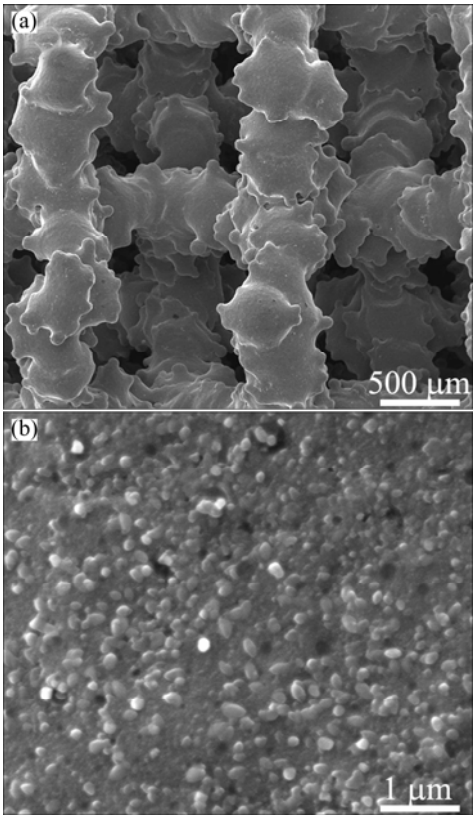

Fig. 2 SEM micrographs of Ti6Al4V scaffold hydrothermally-treated with parameters of sample SB-24h: (a) Lower magnification; (b) Higher magnification

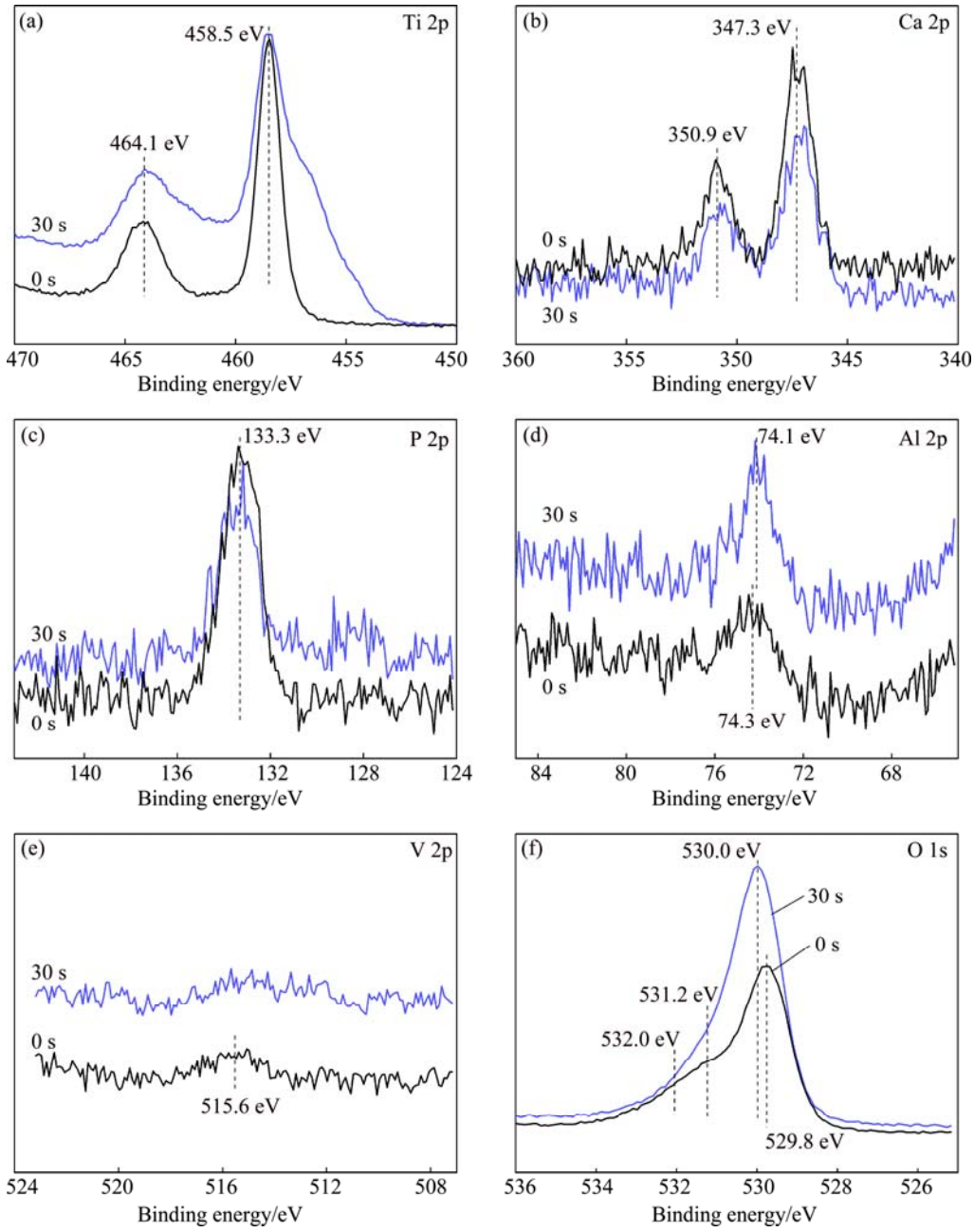

Fig. 3 XPS spectra of sample SB-24h at different sputtering time

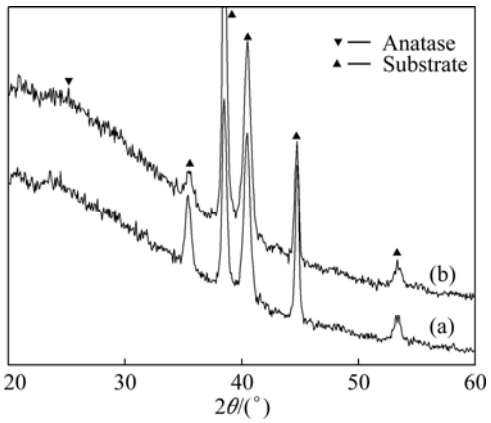

Fig. 4 Grazing-angle XRD patterns of samples SB-16h (a) and SB-24h (b)

Hydrothermal method is widely employed to synthesize TiO_2 and alkaline−earth titanate with high purity, and the mechanism of the reactions has been established as a dissolution−precipitation process [15]. During the hydrothermal treatment of titanium in water, the nanostructured TiO_2 films can be formed on the substrate through the following reactions [15,22]:

$$TiO_2+nH_2O \rightarrow TiO_2{\cdot}nH_2O(gel) \quad (1)$$

$$TiO_2{\cdot}nH_2O(gel) \rightarrow TiO_2+nH_2O \quad (2)$$

$$Ti+2H_2O \rightarrow TiO_2+2H_2\uparrow \quad (3)$$

The alloy elements of Al and V on the sample surface were oxidized during the treatment (Fig. 3). Since the solutions of $CaHPO_4$ and $Ca(H_2PO_4)_2$ are

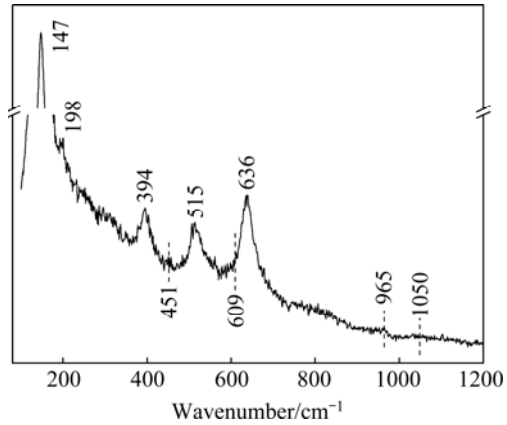

Fig. 5 Raman spectrum of sample SB-72h

slightly acidic after the treatment (pH ~6), it is reasonable that Al is partially dissolved as Al ions in the solutions, but the mechanisms still need a further study. When alkaline−earth metal ions are present in the aqueous system of hydrothermal treatment, titanates will be synthesized:

$$Me^{2+}+TiO_2{\cdot}nH_2O(gel)+2OH^- \rightarrow MeTiO_3+mH_2O \quad (4)$$

The formation of $CaTiO_3$ may provide nucleating sites for calcium phosphates.

In order to verify the phase of calcium phosphate grains in Fig. 1, 50 mmol/L $CaHPO_4{\cdot}2H_2O$ solution was hydrothermally treated at 200 °C for 24 h, washed and dried at 80 °C overnight. XRD analysis indicates that the obtained powder is composed of $CaHPO_4$ and hydroxyapatite, which is consistent with the report that hydroxyapatite nano-crystallites can be prepared by hydrothermal hydrolysis of $CaHPO_4{\cdot}2H_2O$ and $Ca_3(PO_4)_2$ [23]. Therefore, the large particles in Fig. 1(d) are suggested to be hydroxyapatite crystallites.

3.3 Corrosion test

Corrosion resistance of the Ti6Al4V samples was tested by potentiodynamic polarization in the Ca-free HBSS solution (Fig. 6). The polished sample has lower corrosion potential (φ_{corr}) and smaller corrosion current density (J_{corr}) than the hydrothermally-treated sample SB-24h. For the polished sample, a stable passive current density (J_{pass}=2.289 μA/cm^2) and a high pitting potential (φ_{pit}=1.41 V) are obtained after a long range of anodic polarization (Table 3). During the anodic polarization, the dissolution of Al and V elements leads to the increase of anodic current, and the current becomes stable when a resistant titania film is finally formed on the sample surface. Sample SB-24h has a lower pitting potential, but a much lower passive current density (about 1/26 that of the polished sample) than the polished sample. The hydrothermally grown TiO_2−CaP film has effectively improved corrosion resistance of Ti6Al4V alloy, which will impede the corrosion-related release of toxic and carcinogenetic Al and V ions from the alloy substrate. The modified Ti6Al4V alloy is expected to possess better biological properties.

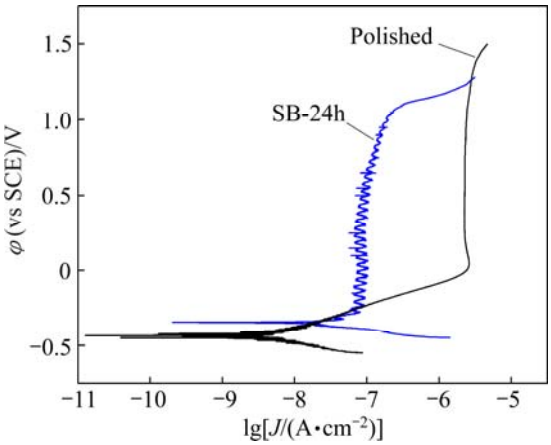

Fig. 6 Potentiodynamic polarization plots of different Ti6Al4V samples

Table 3 Corrosion parameters of Ti6Al4V alloy samples

Sample	J_{corr}/(μA·cm^{-2})	φ_{corr}(vs SCE)/V	φ_{pit} (vs SCE)/V	φ_{pass}/V	J_{pass}/(μA·cm^{-2})
Polished	0.005	−0.43	1.41	1.37	2.289[1)]
SB-24h	0.012	−0.35	1.08	1.36	0.087[1)]

1): Value at middle potential of passivation range, φ_{pass}

4 Conclusions

1) Ti6Al4V alloy was hydrothermally treated in three concentrated calcium phosphate solutions for bioactive surface modification. With the formation of TiO_2−CaP nano-films on the surface, the treated sample has markedly improved corrosion resistance compared with the polished sample.

2) The TiO_2−CaP nano-films were also grown on the strut surface of the Ti6Al4V scaffold prepared by EBM technology. The present work provided a facile bioactive surface modification method suitable for porous biomedical Ti6Al4V alloy.

References

[1] RYAN G, PANDIT A, APATSIDIS D P. Fabrication methods of porous metals for use in orthopaedic applications [J]. Biomaterials, 2006, 27: 2651−2670.

[2] WANG Xiao-hua, LI Jin-shan, HU Rui, KOU Hong-chao, ZHOU Lian. Mechanical properties of porous titanium with different distributions of pore size [J]. Transactions of Nonferrous Metals Society of China, 2013, 23(7): 2317−2322.

[3] LIU Chao, YANG Hai-lin, LI Jian, RUAN Jian-min. Porosity and mechanical properties of biomedical porous Nb−Ti alloy [J]. Transactions of Nonferrous Metals Society of China, 2014, 24(3): 752−757.

[4] HOU Le-gan, LI Li, ZHENG Yu-feng. Effects of ball milling time on porous Ti−3Ag alloy and its apatite-inducing abilities [J]. Transactions of Nonferrous Metals Society of China, 2013, 23(5): 1356−1366.
[5] SU Xu-bin, YANG Yong-qiang, YU Peng, SUN Jian-feng. Development of porous medical implant scaffolds via laser additive manufacturing [J]. Transactions of Nonferrous Metals Society of China, 2012, 22(S1): s181−s187.
[6] LI X, WANG L, YU X M, FENG, Y F, WANG C T, YANG K, SU D. Tantalum coating on porous Ti6Al4V scaffold using chemical vapor deposition and preliminary biological evaluation [J]. Materials Science & Engineering C, 2013, 33: 2987−2994.
[7] LI X, FENG Y F, WANG C T, LI G C, LEI W, ZHANG Z Y, WANG L. Evaluation of biological properties of electron beam melted Ti6Al4V implant with biomimetic coating in vitro and in vivo [J]. PLOS One, 2012, 7(12): e52049.
[8] ZHOU R, WEI D Q, CHENG S, LI B Q, WANG Y M, JIA D C, ZHOU Y, GUO H F. The structure and in vitro apatite formation ability of porous titanium covered bioactive microarc oxidized TiO_2-based coatings containing Si, Na and Ca [J]. Ceramics International, 2014, 40: 501−509.
[9] QU J, LU X, LI D, DING Y H, LENG Y, WENG J, QU S X, FENG B, WKTARI F. Silver/hydroxyapatite composite coatings on porous titanium surfaces by sol−gel method [J]. Journal of Biomedical Materials Research: Part B, 2011, 97: 40−48.
[10] LIN J G, LI Y C, WONG C S, HODGSON P D, WEN C E. Degradation of the strength of porous titanium after alkali and heat treatment [J]. Journal of Alloys and Compounds, 2009, 485: 316−319.
[11] XIONG J Y, LI Y C, WANG X J, HODGSON P, WEN C. Mechanical properties and bioactive surface modification via alkali-heat treatment of a porous Ti−18Nb−4Sn alloy for biomedical applications [J]. Acta Biomaterialia, 2008, 4: 1963−1968.
[12] FU T, LIU B G, ZHOU Y M, WU X M. Sol−gel titania coating on NiTi alloy with a porous titania film as interlayer [J]. Journal of Sol−Gel Science and Technology, 2011, 58: 307−311.
[13] ZHENG C Y, LI S J, TAO X J, HAO Y L, YANG R. Surface modification of Ti−Nb−Zr−Sn alloy by thermal and hydrothermal treatments [J]. Materials Science and Engineering C, 2009, 29: 1245−1251.
[14] CHEN X B, LI Y C, DU PLESSIS J, HODGSON P D, WEN C. Influence of calcium ion deposition on apatite-inducing ability of porous titanium for biomedical applications [J]. Acta Biomaterialia, 2009, 5: 1808−1820.
[15] SHI X L, NAKAGAWA M, KAWACHI G, XU L L, ISHIKAWA K. Surface modification of titanium by hydrothermal treatment in Mg-containing solution and early osteoblast responses [J]. Journal of Materials Science: Materials in Medicine, 2012, 23: 1281−1290.
[16] NAKAGAWA M, ZHANG L, UDOH K, MATSUYA S, ISHIKAWA K. Effects of hydrothermal treatment with $CaCl_2$ solution on surface property and cell response of titanium implants [J]. Journal of Materials Science: Materials in Medicine, 2005, 16: 985−991.
[17] CHUSUEI C C, GOODMAN D W, VAN STIPDONK M J, JUSTES D R, SCHWEIKERT E A. Calcium phosphate phase identification using XPS and time-of-flight cluster SIMS [J]. Analytical Chemistry, 1999, 71: 149−153.
[18] WAGNER C D, RIGGS W M, DAVIS L E, MOULDER J F. Handbook of X-ray photoelectron spectroscopy [M]. Minnesota: Perkin-Elmer Corporation, 1979.
[19] CHANG H, HUANG P J. Thermo-Raman studies on anatase and rutile [J]. Journal of Raman Spectroscopy, 1998, 29: 97−102.
[20] GU Y W, TAY B Y, LIM C S, YONG M S. Biomimetic deposition of apatite coating on surface-modified NiTi alloy [J]. Biomaterials, 2005, 26: 6916−6923.
[21] SABER-SAMANDARI S, ALAMARA K. Calcium phosphate coatings: Morphology, micro-structure and mechanical properties [J]. Ceramics International, 2014, 40: 563−572.
[22] HAMADA K, KON M, HANAWA T, YOKOYAMA K, MIYAMOTO Y, ASAOKA K. Hydrothermal modification of titanium surface in calcium solutions [J]. Biomaterials, 2002, 23: 2265−2272.
[23] WATANABE T, KAWACHI G, KAMITAKAHARA M, KIKUTA K, OHTSUKI C. Formation of needle-like hydroxyapatite by hydrothermal treatment of $CaHPO_4{\cdot}2H_2O$ combined with β-$Ca_3(PO_4)_2$ [J]. Journal of the Ceramic Society of Japan, 2009, 117: 759−764.

Ti6Al4V 合金上 TiO_2−CaP 纳米薄膜的简易水热合成

付 涛[1]，李红伟[2]，孙见敏[1]，李 纲[3]，李 雯[2]，张红梅[1]

1. 西安交通大学 生命科学与技术学院 生物医学信息工程教育部重点实验室，西安 710049；
2. 长安大学 材料科学与工程学院，西安 710064；
3. 西北有色金属研究院 金属多孔材料国家重点实验室，西安 710016

摘 要：采用高浓度 $Ca_3(PO_4)_2$、$CaHPO_4$ 和 $Ca(H_2PO_4)_2$ 溶液对 Ti6Al4V 合金进行水热处理，以进行生物活性表面改性。经过处理的试样表面覆盖的薄膜由尺寸为 60~240 nm 的纳米颗粒组成。这种薄膜也能在电子束熔融技术制备的 Ti6Al4V 支架上生长。X 射线光电子能谱分析表明，试样表面钛元素以 TiO_2 形式存在，钙和磷元素以磷酸钙形式存在。X 射线衍射和拉曼光谱分析表明，试样表面层由锐钛矿 TiO_2 和羟基磷灰石组成。在无钙 Hank's 平衡盐液中的动电位极化实验表明，水热处理试样的耐蚀性比抛光试样的显著提高。本研究提供了易于操作、处理温度低、腐蚀性低的生物活性表面改性方法，此方法可用于生物医用多孔 Ti6Al4V 合金的表面改性。

关键词：钛；TiO_2；磷酸钙；水热处理；腐蚀

(Edited by Wei-ping CHEN)